# Investigating the Flight of Sycamore Seeds using Origami Models and a 3D Simulation

Amber Covington, Jodie Kelly, Robert Smith, David Taylor & Joe Fretwell
Physics Bridge Project, Team 1, Prof. J. Girkin
Submitted: June 19, 2020, Date of Experiments: June 10 - 12, 2020

The dynamics of flight and the variables affecting the flight of sycamore seeds were investigated by constructing paper origami models, while the airflow around an actual sycamore seed was investigated using a 3D fluid simulation. The gsm (grams per square metre) of paper used for the origami models and the size of the model were varied individually, with the flight analyzed using slow motion video. It was found that increasing the gsm of the model was directly correlated to an increasing terminal velocity and that increasing the size was directly correlated to a smaller cone angle and a lower angular velocity. No correlation between the gsm and cone angle, gsm and angular velocity or the size and the terminal velocity was found. The dynamics of flight were evaluated using flow diagrams from the 3D simulation.

## I. INTRODUCTION

Seed dispersal is a crucial factor in the spread of a trees genetics. The likelihood of seed survival is greater when the seed lands far from its parent, as there is less competition for nutrients and sunlight with the adult tree. The seeds of the sycamore tree have evolved to have a single wing protruding from the nut, which utilizes aerodynamic effects to spin, therefore increasing lift and slowing the descent of the seed to maximise dispersal distance.

Analysis of these highly effective flying seeds could have applications in various fields of engineering. Notable examples include the design of more efficient wind turbine and helicopter blades.

Slow motion video was taken of the flight of origami and real sycamore seeds, and analysed to calculate the terminal velocity, angular velocity and cone angle of its flight. The aim was to investigate the trends in these properties as the area and gsm (grams per square metre) of the paper seeds were varied. The effectiveness of the origami sycamore seeds was then compared to that of real sycamore seeds. A 3D model of a real sycamore seed in the CAD software SolidWorks was used to investigate the fluid flow around the seed as it fell.

## II. THEORY

Objects fall at terminal velocity when there is no resultant force acting on it, meaning the weight is equal to the drag force. Weight is given by

$$W = mg \tag{1}$$

with $W$ being the weight, $m$ being the mass and $g$ being the local gravitational acceleration. Drag is given by [1]

$$D = \frac{C_d \rho v^2 A}{2} \tag{2}$$

with $D$ being the drag force, $\rho$ being the density of air, $v$ being the velocity relative to the surrounding air, $A$ being wing area and $C_d$ being the drag coefficient, which depends on if you measure the wing area as projected in the direction of wind or non-projected. $C_d$ is also dependent on the shape of the object, the flow conditions and surface roughness, and will change depending on how the seed is spinning. Equating equations 1 and 2 and solving for terminal velocity we get

$$v_{ter} = \sqrt{\frac{2mg}{C_d \rho A}} \tag{3}$$

with $v_{ter}$ being the terminal velocity.

The angular and vertical movements of sycamore seeds are governed by many interdependent factors such as mass, wing area, cone angle, pitching angle, moment of inertia and gyroscopic effects [2]. The moment of inertia is important in understanding the rotational mechanics of the flight and is given by

$$I = \int_0^m r^2 dm \tag{4}$$

with $I$ being the moment of inertia and $r$ being the distance to the mass element $dm$, where a larger moment of inertia corresponds to a slower angular velocity.

As the wing falls, it causes displacement of air molecules beneath it, and by Newton's third law a force acts upwards on the wing generating lift. Another factor generating lift is the formation of a leading edge vortex (LEV) [3], in which the leading edge creates a stable vortex on the wing as it rotates. In turn, this creates an area of low pressure on top of the wing, inducing a pressure difference (called pressure drag, or form drag) which results in an a upward lift force.

## III. METHODS

Two different independent variables, initial paper area (before folded into the seed) and paper mass were tested using a similar method to find how they affect the flight of sycamore seeds. Several pieces of rectangular paper with side lengths of ratio 1:3 were folded into the shape of a sycamore seed using the same folding technique [4]. Figure 1 shows the appearance of the origami seed and its key features. We made sure to keep the folds as flat as possible by running a blunt object over them to maintain uniformity of the models, and thus reduce random error. When changing the paper area, the same grade of paper - 80 gsm - was used, and when changing the paper mass, a constant area of paper, 3 cm by 9 cm, was used. The seeds were filmed in natural lighting and the paper had a contrasting colour to the background to improve visibility of the seed in the video for analysis.

A side view of the falling sycamore seed was taken by a slow motion camera filming at 120 frames per second placed roughly 1.5 m away from the initial dropping point of the sycamore seed. The camera was placed perpendicular to the direction of travel of the seed and at a large distance from the dropping point in order to minimise parallax error when analysing the video frames.

A calibration was performed in order to find the centimetre to pixel ratio. This was done by creating a scale of separations of known distance next to the falling sycamore seed. The intensity profile of the scaled lines could then be drawn using ImageJ [5] and the average distance between the intensity peaks could be taken. This distance in pixels could then be used along with the known separation of the scale to calculate the length of one pixel in centimeters.

Seeds were dropped from a height of roughly 2 m and orientated at a 45 degree angle with the nut pointed towards the ceiling as this condition allowed the seed to reach a stable spinning state before entering the field of view of the camera. The environment that the seeds were dropped in had minimal air currents, achieved by keeping all windows and doors closed.

The slow motion videos of the seeds falling in their stable states were then split in to their individual frames as png images using FFMPEG software, as png compression is lossless, to allow for higher precision during analysis. The video frames were then uploaded into ImageJ as a stack, enabling easy scrolling between the frames. Using ImageJ the distance the seed travelled could be measured with large accuracy by using the draw line tool between two different frames of the seed's descent and reading the difference in the y-coordinates. This was used with the difference in frame number to calculate the terminal velocity of the seed.

The angular velocity of the falling seeds was calculated in ImageJ by measuring several complete rotations over a known number of frames and taking an average, mitigating the error introduced by the seed drifting during its flight. The cone angle, shown in figure 2, was also measured using the line tool in ImageJ to draw a line along the length of the seed when parallel to the frame of the camera, giving the angle the seed made with the horizontal, from which the cone angle was calculated. The cone angle was measured at three different points throughout its flight and an average was taken to minimise the error from the seed rocking as it fell.

**3D model:** In order to create the 3D model on SolidWorks we used a digital micrometer to measure the dimensions of real sycamore seeds across 18 different features, such as total length and wing width. We zeroed the micrometer after each measurement to prevent systematic error. The model was constructed based on the average of these results to reduce random error and account for anomalous variations in individual seeds.

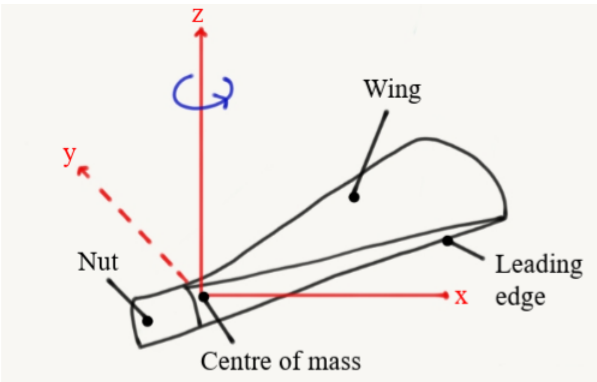


**Figure 1:** Diagram of an origami sycamore seed mid-flight.

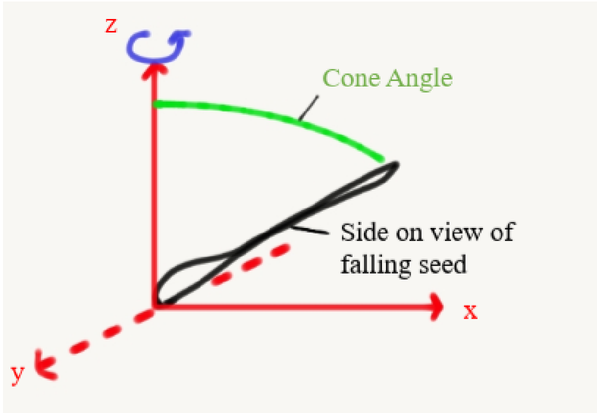


**Figure 2:** Diagram of how the cone angle is measured mid flight.

## IV. RESULTS

**Changing the gsm:** Using Spearman's rank test with figures 4 and 6 indicates that the gsm of the paper used to create the sycamore seed model is correlated with its terminal velocity, whilst there is no correlation between the gsm and the angular velocity or cone angle of the model.

The application of Spearman's rank to the values shown in figure 4 gave rank coefficients of $-0.098$ and $-0.036$ for the cone angle and angular velocity respectively. The critical value for these 15 data points was $0.446$ at the $95\%$ confidence level, hence since the rank coefficients have a smaller magnitude than this, the null hypothesis was accepted. There is no correlation between the gsm and angular velocity nor cone angle.

However, Spearman's rank gave a rank coefficient of $0.986$ for the data in figure 5, hence the null hypothesis was rejected. There is a positive correlation between the gsm and terminal velocity, since the rank coefficient is positive and greater than the critical value of $0.446$. The graph strongly indicates a linear fit within the tested range for this data, further supported by a linear regression calculation. This graph has an R-Squared value of $0.866$ - a relatively strong linear correlation.

**Changing the area:** Spearman's rank was also applied to figures 5 and 6, to give rank coefficients of $-1.000$, $-1.000$ and $0.314$ for the angular velocity, cone angle and terminal velocity respectively. A critical value of $0.829$ was taken at the $95\%$ confidence level for the 6 sets of data. As a result, since the rank coefficient of the terminal velocity and area is less than the critical value, the null hypothesis is accepted and there is no linear correlation between the terminal velocity and the area. The null hypothesis is rejected for the angular velocity and cone angle data - there is a negative correlation between the angular velocity and area, and the cone angle and area, since the rank coefficient is negative for both variables and greater than the critical value. Calculating R-Squared values for both data sets gives $R = 0.840$ for the angular velocity, and $R = 0.984$ for the cone angle. These both indicate strong linear correlations for the measured data set.

**Link to YouTube playlist** $\rightarrow$ shorturl.at/oJK02 This playlist shows some animations of flowlines and some slow motion videos of the origami seeds during their flight.

**Real Seed and 3D model:** From analysing the video of the real sycamore seeds we found that the terminal velocity was $47 \pm 7$ cm s$^{-1}$, the angular speed was $160 \pm 4$ rad s$^{-1}$

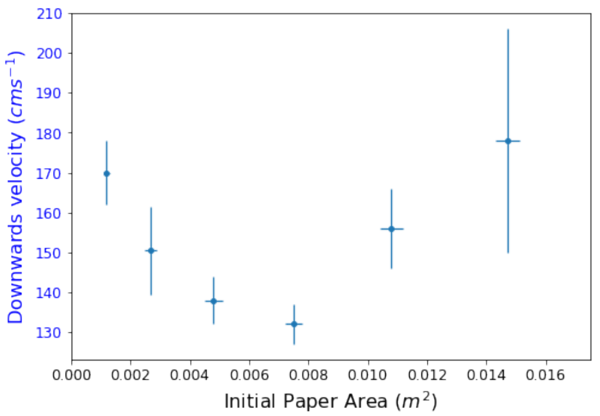


**Figure 3:** Downwards velocity plotted against the paper area.

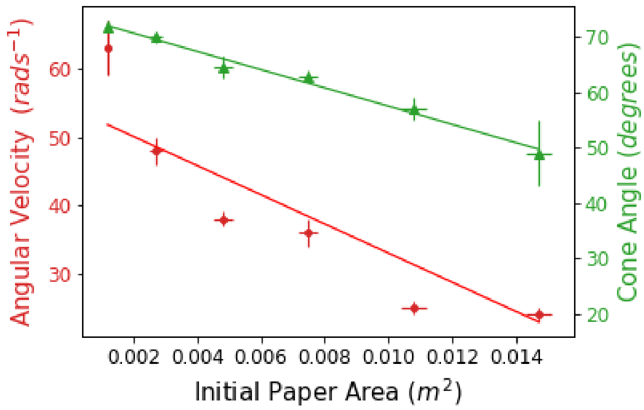


**Figure 5:** Angular velocity (circles) and Cone angle (triangles) plotted against the initial paper area.

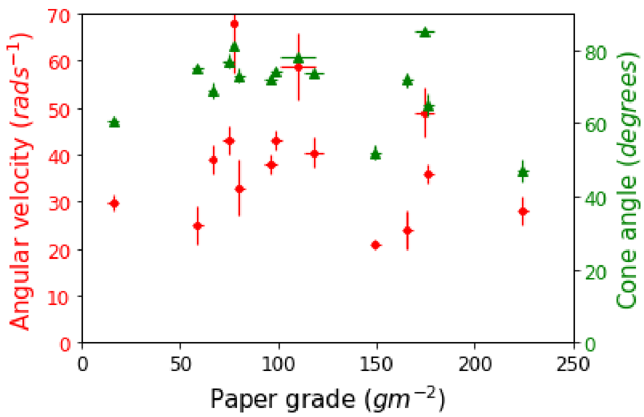


**Figure 4:** Angular velocity (circles) and Cone angle (triangles) plotted against the paper grade.

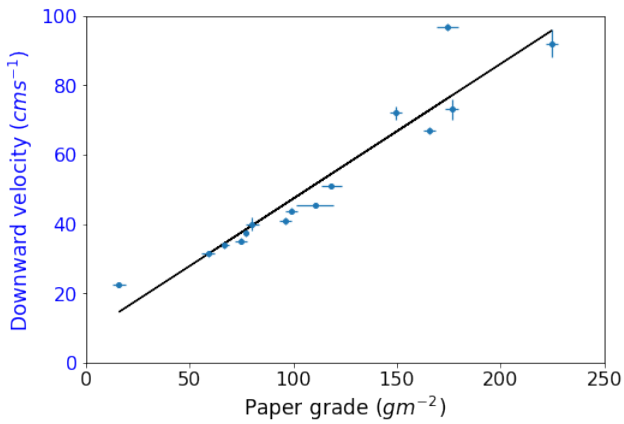


**Figure 6:** Downwards velocity plotted against the initial paper grade.

and cone angle was $73 \pm 3$ degrees.The average length of the sycamore seed was measured to be $43.65 \pm 0.01$ mm. Using $v_{rot} = \omega r = \omega L_{seed}/2$ with $v_{rot}$ being rotational speed, $\omega$ being the angular velocity and $L_{seed}$ being the length of seed measured from nut to tip, we found that $v_{rot}$ was $3.49 \pm 0.09$ cm s$^{-1}$. Reversing the directions of the falling and rotating velocities gives the wind speed. Using these values and rotating the model up to the cone angle, we get the input parameters for the fluid simulation package on SolidWorks.

## V. DISCUSSION

**Changing gsm:** The relation of the gsm with the terminal velocity as seen in figure 6 can likely be explained by the increase in mass of the seed, with negligible change in the shape. The $C_d$ value is not expected to change since the flow conditions would not change significantly, due to a similar surface roughness. The formation of the LEV is unaffected. As a result, the lift on the seed is not changed significantly but the weight is greater, hence using equation 3 a larger terminal velocity is reached before the forces are in balance.

When the gsm of the paper is changed, the moment of inertia as described in equation 4 does not significantly change, since all parts of the seed are equally altered, and the majority of the mass remains in the nut, which is close to the axis of rotation. However, since the larger mass of paper has a greater weight, it will fall somewhat faster than paper with a smaller mass, generating more lift on the wing. It is also to be noted that, generally, the higher the gsm the stiffer the wing - this means that the upward force of the air resistance is greater on higher gsm paper, resulting in a larger cone angle. As a result, the rate of rotation of the paper has a complex relation with the mass of the seed, as seen in figure 4.

Figure 4 also shows that the angular velocity and cone angle have a somewhat random nature to them; this could be due to slight variations in the air currents, resulting in a random error. Lastly, the paper used was not all the same in the experiments, and varied in texture. These changes in texture would affect the formation of the LEV and the $C_d$ value of the seed, creating the random variation in values obtained.

**Changing size:** Figure 5 shows a general negative trend in the cone angle and angular velocity with increasing seed dimensions. There is, however, no clear correlation between the terminal velocity and the seed dimensions, shown in Figure 6.

Smaller seeds have a smaller moment of inertia as they have less mass, which is also distributed closer to the rotation axis because of the smaller wing size. This allows for a greater angular velocity for a given transfer of gravitational potential energy into kinetic energy, resulting in faster rotation. This is evident in our graph.

A lower angular velocity decreases the gyroscopic effect, based on inertia and angular momentum, on the rotating seed, reducing the stability of the angle of rotation about the axis. A larger wing area also produces more upward force from drag as it falls. The increased upward force on the wing, coupled with the decreased stability, rotates the wing upwards into its position with a lower cone angle, as is evident in figure 5.

The lack of a simple correlation in the velocity measurement is due to the complex aerodynamic interactions of all the changing variables. A larger wing area has a larger leading edge to produce a longer LEV and can experience more drag as it falls. This larger wing, however, rotates slower so this vortex is weaker, and there is a smaller cone angle so the area of the wing contributing to drag will be smaller. There are many factors contributing to the terminal velocity of a seed of a given size, and it is not clear from the data gathered which is most prominent. Indeed the most relevant factor may even change as one changes the seed mass and dimension. It is also possible that there is a non-linear relationship present in the data (see the parabolic nature of figure 3) so further investigation on this specific data set, perhaps over a wider range of sizes, could be more successful in determining a more nuanced relationship between variables affecting the flight of a sycamore seed.

**Comparing model to actual sycamore seed:** The dimensions of the origami seed was chosen to be as close as possible to the actual sycamore seed whilst remaining visible from a reasonable distance by the camera. The terminal velocity of the actual sycamore seed ($47 \pm 7$ cm $s^{-1}$) is of a similar order to the terminal velocity measured when changing the gsm of the paper, in figure 5, but is considerably less than that measured when changing the initial paper area. The cone angle of the models were similar in magnitude to the real sycamore seed ($73 \pm 3$ degrees), as in figures 4 and 5, approximately corresponding to a median cone angle when changing the gsm of the paper, and a small initial paper area. Lastly, the angular velocity of the real sycamore seed ($160 \pm 4$ rad $s^{-1}$) is considerably greater than the models.

The differences in the parameters of the flight of the origami models compared to the real sycamore seed is likely to be primarily due to a difference in shape. The real sycamore seed has a more curved wing compared to our models and smooth edges and turns. In addition, a real sycamore seed has veins along the leading edge of its wing in the direction of airflow whilst rotating, which modifies the air flow over the wing. The ratio of the mass of the nut of the real sycamore seed to the mass of the wing will also differ from the origami model. Lastly, it is to be noted that terminal velocity was assumed to have been reached in the experiments but, especially with higher mass models, this may not always have been the case.

**3D model:** In the model exact numbers do not matter, as the use of approximate values yield similar conditions for the flight. This is why it does not matter that we took the rotation speed at the middle of the wing. From Figure 7, we see the formation of the LEV, where the blue vectors representing slow airflow are found in the middle of the vortex and fast airflow, represented by red vectors, flow around this vortex.

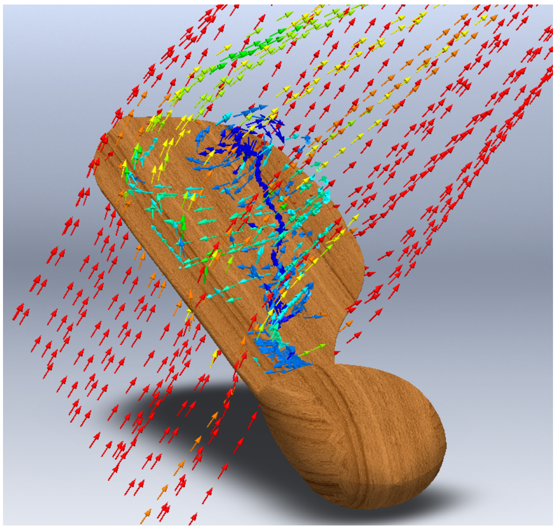

**Figure 7:** Vector flow of particle trajectory on a model of a sycamore seed, red lines indicate fast flow and deep blue indicate slow flow

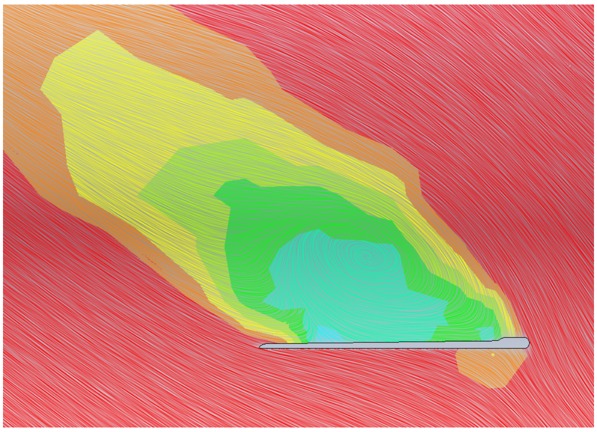

**Figure 8:** Velocity flowlines on a cross section of the sycamore seed model, red areas indicate fast flow and blue indicates slow flow

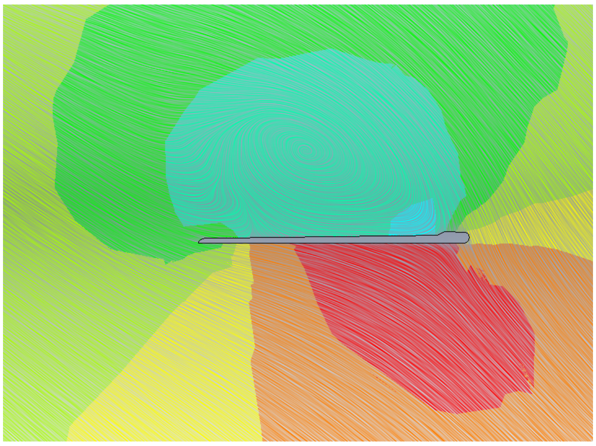

**Figure 9:** Relative pressure flowlines on a cross section of the sycamore seed model, red areas indicates high pressure and blue areas indicates low pressure

We can study the velocity flowlines around a cross-section of the wing, where the flowlines are shown in Figure 8. We see that the slowest airflow is in the middle of the vortex, and a trail of slower air which goes past the end of the wing caused by the vortex is pulling on the air behind it from here. The slower patch of air found below the leading edge of the wing is caused by the skin friction of the wing as it cuts through the air.

SolidWorks allows us to see the pressure differences acting on the section of the wing shown in Figure 9. In this, we see a high-pressure zone formed under the leading edge, caused by the compression of flowlines and a low-pressure zone spread across the top of the wing, due to the vortex. This difference in pressure causes pressure drag, generating more lift.

This pressure difference also affects the cone angle by generating a torque acting against weight, decreasing the cone angle. The skew of the high-pressure area under the wing towards the leading edge creates a torque, which determines the pitch angle.

The component of the lift force that is directed towards the axis of rotation is responsible for the centripetal force. The rotational velocity generates the LEV, which generates pressure drag. This in turn contributes to the centripetal force required for the rotation, so the seed forms a stable rotation with the additional lift force causing a slower terminal velocity.

## VI. EVALUATION

Due to the restrictions in place as a result of the COVID-19 pandemic, we as a group were each at our own homes, performing experiments separately. This limited the available equipment and meant extra steps were required in our method to ensure results could be adequately compared.

The main limiting feature of the origami experiments was the video camera. If we had access to a high quality slow motion camera with uniform white lighting we would expect to get more precise measurements. A higher frame rate would give more accurate results with greater precision for angular and terminal velocity, and the high frame quality would allow us to determine cone angle more accurately. Having a set up involving multiple high speed cameras could perhaps allow us to measure pitching angle, giving more insight into the mechanics of flight. [6]

Having access to paper with the same surface roughness and varying gsm so as to maintain a constant mass when changing the size of the seed would show how the area affects the flight, independent from mass. We could have also changed the experimental variables in the 3D model to check that the dynamics of flight changed in a way as to match our conclusions.

Access to a more controlled environment in terms of air flow and pressure would have limited the differences in flight path when dropping the seeds reducing random error. An example of this would be a chamber excluding ventilation, perhaps built for studying the descent of other flying objects [7].

## VII. CONCLUSIONS

Analysis using slow motion videos of origami sycamore seeds showed that the flight depends on the area of the seed and its mass- such that the angular velocity and cone angle of the seeds have a negative, linear correlation with the initial paper area. In addition, the terminal velocity and paper grade have a positive, linear correlation. However, the terminal velocity with paper area, and the angular velocity/cone angle with the paper grade have a more complex relation, but no notable correlation.

The dynamics of flight were investigated using flowline diagrams from a 3D simulation, giving possible explanations of the mechanisms behind flight, involving the formation of an LEV and overal

From comparison of our models with a real sycamore seed, evolution has clearly found the most efficient method of sycamore seed dispersal, with the optimal size, shape and mass to create sufficient lift to reduce the speed of descent of the seed and maximise seed dispersal.

**Acknowledgments**

Much thanks is due to our project leader Prof JM Girkin, FInstP, FOSA for his constant guidance, insightful advice and enthusiastic interest in all that we undertook.

**References**

[1] Barnes W. McCormick,*'AERODYNAMICS, AERONAUTICS, AND FLIGHT MECHANICS SECOND EDITION'* (1995), page 28
[2] Ralph D. Lorenz, *'Spinning flight'*, (2006), page 274
[3] Lee S.J, Lee E.J & Sohn M.H, *'Mechanism of autorotation flight of maple samaras (Acer palmatum)'*, (2014), Exp Fluids 55, 1718
[4] Origamido Studios, *'Simple Origami Maple Seed'*,(2018) Accessed on: 17/06/2020
[5] ImageJ Version 1.53b (31/05/2020) Accessed on: 16/06/2020
[6] Kapil Varshney, Song Chang and Z Jane Wang, *'The kinematics of falling maple seeds and the initial transition to a helical motion'*, (2011)
[7] R.A.Stevenson, D.Evangelista, C.V.Looy, *Paleobiology*, (2015), 41, 205-225
[8] I.G.Hughes and T.P.Hase, *'Measurements and their Uncertainties'*, Oxford University Press, US (2010), chapters 2 and 4

### A. Error Appendix

For a single-variable function the functional approach [7] gives the error on $A$ as,

$$\alpha_A =\mid f(A+\alpha) - f(A) \mid \tag{5}$$

This was used with the error on any measurements taken to extrapolate the error bars on Figures 3,4,5 and 6. For the cone angle, downwards velocity and angular velocity many repeats were taken and the standard error used to quantify the distribution of results,

$$\alpha_{S.E} = \frac{\sigma}{\sqrt{N}} \tag{6}$$

When combining errors for $Z$ the following propagation functions were used [7] ;

$$\alpha_Z = \sqrt{(\alpha_A)^2 + (\alpha_B)^2} \tag{7}$$

for addition functions and

$$\alpha_Z = Z\sqrt{(\frac{\alpha_A}{A})^2 + (\frac{\alpha_B}{B})^2} \tag{8}$$

for multiplicative ones. Both shown for functions of two variables. These were used propagating errors through individual measurements.

### B. Risk Assessment

This was electronically signed prior to the beginning of the experiment by all members of the group. A copy can be found in the Microsoft Teams group ”Bridge Project Team 1 Flying Trees” → Class Notebook → Collaboration Space → Final report → Risk assessment